

Querkopf is a key marker of self-renewal and multipotency of adult neural stem cells

Bilal N. Sheikh^{1,2}, Mathew P. Dixon¹, Tim Thomas^{1,2,*} and Anne K. Voss^{1,2,*}

¹The Walter and Eliza Hall Institute of Medical Research, Parkville 3050, Victoria, Australia

²Department of Medical Biology, University of Melbourne, Parkville, Victoria, Australia

*These authors co-supervised this project and contributed equally to this work

†Authors for correspondence (avoss@wehi.edu.au; tthomas@wehi.edu.au)

Accepted 22 July 2011

Journal of Cell Science 125, 295–309

© 2011. Published by The Company of Biologists Ltd

doi: 10.1242/jcs.077271

Summary

Adult neural stem cells (NSCs) reside in the subventricular zone (SVZ) and produce neurons throughout life. Although their regenerative potential has kindled much interest, few factors regulating NSCs *in vivo* are known. Among these is the histone acetyltransferase querkopf (QKF, also known as MYST4, MORF, KAT6B), which is strongly expressed in a small subset of cells in the neurogenic subventricular zone. However, the relationship between *Qkf* gene expression and the hierarchical levels within the neurogenic lineage is currently unknown. We show here that the 10% of SVZ cells with the highest *Qkf* expression possess the defining NSC characteristics of multipotency and self-renewal and express markers previously shown to enrich for NSCs. A fraction of cells expressing *Qkf* at medium to high levels is enriched for multipotent progenitor cells with limited self-renewal, followed by a population containing migrating neuroblasts. Cells low in *Qkf* promoter activity are predominantly ependymal cells. In addition, we show that mice deficient for *Bmi1*, a central regulator of NSC self-renewal, show an age-dependent decrease in the strongest *Qkf*-expressing cell population in the SVZ. Our results show a strong relationship between *Qkf* promoter activity and stem cell characteristics, and a progressive decrease in *Qkf* gene activity as lineage commitment and differentiation proceed *in vivo*.

Key words: MYST, Epigenetics, Neurogenesis, Neural stem cells, HAT, Histone acetyltransferase, Fluorescence-activated cell sorting, Polycomb

Introduction

Adult neural stem cells (NSCs) are present in the subventricular zone (SVZ) and the subgranular layer of the hippocampus and are a source of new neurons throughout life (Zhao et al., 2008). SVZ NSCs give rise to transit amplifying cells, which in turn produce neuroblasts that migrate to the olfactory bulbs and differentiate into olfactory interneurons (Lois et al., 1996). SVZ NSCs have been induced to differentiate into an array of different neural cell types, both *in vivo* and *in vitro* (Curtis et al., 2003; Lois and Alvarez-Buylla, 1993). NSCs have therefore aroused great interest, as they hold much promise for the generation of new therapies for neurodegenerative disorders and neural injury. However, two major issues have hindered progress in the field. First, it has been difficult to isolate a pure population of NSCs in their most primitive state. Although some markers are available for the enrichment of NSCs, a definitive marker for NSCs remains to be defined. Second, in order to direct differentiation of NSCs into specific neuronal cell types, which would ideally include cell types not normally formed by NSCs, a greater understanding of factors underlying lineage commitment and hierarchy is required.

NSCs have been shown to express a number of genes including intracellular proteins such as glial fibrillary acidic protein (GFAP), nestin and inhibitor of DNA binding 1 (Id1) (Doetsch et al., 1999; Mignone et al., 2004; Nam and Benezra, 2009), cell surface proteins such as SSEA-1 (also known as FUT4 and LeX) and CD133 (Capela and Temple, 2002; Coskun et al., 2008; Beckervordersandforth et al., 2010), and low levels of heat stable

antigen (HSA; HSA is also known as CD24). NSCs also show little affinity for the lectin peanut agglutinin (PNA) (Rietze et al., 2001). Although some of these characteristics have been used to isolate cell fractions enriched for NSCs, most of the markers are expressed strongly in other cells in the brain, whereas others only mark a subset of NSCs. For example, GFAP is expressed by both NSCs and differentiated astrocytes. Of note, none of the markers currently in use to enrich for or to identify NSCs play a non-redundant role in adult NSC biology. We show here that high levels of querkopf (*Qkf*; also known as *Kat6b* and *Myst4*) expression identifies multipotent, self-renewing NSCs.

We have previously shown that a lack of the MYST-family histone acetyltransferase, QKF, leads to defects in the establishment and self-renewal of adult NSCs and consequently to a progressive defect in adult neurogenesis (Merson et al., 2006; Rietze et al., 2001). Remarkably, in humans loss of only one allele of *MYST4* (*QKF*) leads to intellectual disability (Kraft et al., 2011; Clayton-Smith et al., 2011). Unlike other histone acetyltransferases, the expression of *Qkf* is both spatially and temporally regulated, and strong *Qkf* expression is localized to neurogenic regions both during development and in the adult (Merson et al., 2006; Thomas et al., 2000). We observed strong expression of *Qkf* gene in a small subset of neurogenic SVZ cells, raising the question of whether there is a relationship between *Qkf* gene expression levels and cell identity. Using *Qkf*-GFP transgenic mice to trace levels of *Qkf* gene activity, we show that the strongest *Qkf*-GFP-expressing cells possess all NSC characteristics, namely multipotency and self-renewal.

Moreover, we show a remarkable relationship between levels of *Qkf*-GFP expression and progression in neuronal lineage differentiation.

Results

Characterizing *Qkf*-GFP reporter expression in transgenic mouse lines

Qkf-GFP bacterial artificial chromosome (BAC) transgenic mice were generated by microinjection of the BAC vector depicted in Fig. 1A into fertilized oocytes. The BAC vector contained an *eGFP* reporter inserted at the start codon of *Qkf* in exon 1. In addition, the BAC contained genomic sequence from 67 kb upstream to 130 kb downstream of the *Qkf* start codon. Offspring of the BAC transgenic founder mice were screened for expression of the GFP reporter between embryonic day (E)9.0 and E12.5. At E9.5 the endogenous *Qkf* gene and the *Qkf*-GFP transgene were expressed ubiquitously (supplementary material Fig. S1A,B). A total of 19 independent founder *Qkf*-GFP reporter lines were generated. The seven strongest GFP-expressing lines were kept for further analysis.

The presence of GFP reporter expression was confirmed by immunohistochemistry on neurospheres from *Qkf*-GFP transgenic and wild-type littermates. *Qkf*-GFP transgenic cells attached to a laminin substrate stained strongly for GFP, which was absent in wild-type cells (supplementary material Fig. S1C-F).

To determine the mRNA products of the *Qkf*-GFP transgene, a northern blot analysis of RNA isolated from the adult brains of all seven *Qkf*-GFP transgenic lines was performed. Wild-type adult brain RNA and E12.5 RNA were used as controls. *Qkf* probe no. 19 was used to determine endogenous *Qkf* levels. This probe hybridizes to the 5'UTR (untranslated region) and to part of the first coding exon of *Qkf*, both 5' and 3' of the *GFP* insertion site (see Fig. 1A). Consistent with previous studies, *Qkf* transcripts of 1 kb and 7.2 kb were present in the wild-type adult brain (supplementary material Fig. S1G) (Thomas et al., 2000). The same transcripts were also present at similar levels in the *Qkf*-GFP adult brains, suggesting that the endogenous *Qkf* gene was functionally normal. The E12.5 embryo expressed an additional 7.7 kb message, which has been previously observed (Thomas et al., 2000). Using a 668 bp *GFP* probe, messages between 1.3 kb and 1.8 kb were detected in the *Qkf*-GFP transgenic, but not in wild-type samples, with a 1.5 kb mRNA being the most prominent. These RNA species were of the expected size: 1079 bp *GFP* sequence, 113 bp 5'UTR, 35 bp 3'UTR and 50–250 bp poly(A) tail. The 1.5 kb and 1.8 kb messages also hybridized to *Qkf* probe no.19 because of the presence of *Qkf* 5'UTR sequence in the *GFP* mRNAs. In addition, a 1.1 kb transcript was specifically detected by *Qkf* probe no. 19 in the *Qkf*-GFP brain RNA. This transcript was not detected by the *GFP* probe in any wild-type samples. It is therefore likely to be an aberrant splice product of the *Qkf*-GFP transgene, which does not contain the *GFP* coding sequence.

The *Qkf*-GFP transgene activity reflects wild-type *Qkf* gene expression levels

To determine the accuracy of the *Qkf*-GFP reporter in representing the wild-type *Qkf* locus, in situ hybridization was carried out probing for *GFP* and endogenous *Qkf* in brain sections from all seven transgenic lines (example shown in Fig. 1B–G). To distinguish wild-type endogenous *Qkf* from *Qkf*-GFP transgenic

transcripts, a *Qkf* probe (*Qkf* 1332) that hybridizes to exon 16, which is absent from the transgene, was used. Endogenous wild-type *Qkf* mRNA was expressed strongly in the SVZ (Fig. 1B) as previously described (Merson et al., 2006). In particular, a small number of cells within the subependymal layer of the SVZ expressed *Qkf* at high levels (Fig. 1F). Similarly, in an adjacent slide of the same brain, *GFP* mRNA was strongly expressed in specific cells (Fig. 1C,G). The complex pattern of *Qkf* gene expression in the mid-gestation embryo (Thomas et al., 2000) was also faithfully reproduced by the *Qkf*-GFP transgene, with strong expression domains in the developing telencephalon, eyelids, cornea, retina, the lateral aspects of the lens, nasal epithelium, tongue and developing teeth (supplementary material Fig. S1H–I). Taken together, our results suggest that *Qkf*-GFP transgene expression accurately depicts endogenous *Qkf* promoter activity pattern in all seven transgenic lines.

To ensure that *Qkf*-GFP expression levels quantitatively reflect levels of endogenous wild-type *Qkf*, cells from E12.5 embryos from three independent transgenic lines were sorted according to their level of GFP expression by fluorescence-activated cell sorting (FACS). After selecting for single live cells and excluding debris (Fig. 1H), four cell fractions were collected on the basis of their *Qkf*-GFP reporter expression, with the highest 10% *Qkf*-GFP-positive cells designated *Qkf*-GFP high (*Qkf*-GFP^{Hi}). The next three fractions containing 30% of cells each were designated *Qkf*-GFP medium-high (*Qkf*-GFP^{MedHi}), *Qkf*-GFP medium-low (*Qkf*-GFP^{MedLo}), and *Qkf*-GFP low (*Qkf*-GFP^{Lo}; Fig. 1I). Endogenous *Qkf* mRNA expression levels were assayed. In all instances examined, *Qkf*-GFP expression levels correlated strongly with endogenous *Qkf* expression levels ($r=0.9619$, $P<0.0001$, $n=3$ animals; Fig. 1J–L). On average, *Qkf*-GFP^{MedHi} cells had 40% less endogenous *Qkf* expression than *Qkf*-GFP^{Hi} cells ($P<0.0001$). Similarly, *Qkf*-GFP^{Hi} cells had more than twice the amount of endogenous *Qkf* expression than *Qkf*-GFP^{MedLo}, and five-times more *Qkf* expression than the *Qkf*-GFP^{Lo} population ($P<0.0001$). This result and the in situ hybridization data demonstrate that the *GFP* transgene expression under the *Qkf* promoter accurately portrays endogenous *Qkf* expression levels.

To determine whether there is a relationship between *Qkf* promoter activity and neurogenic cell identity in the SVZ, we carried out in vivo cell cycle studies and imaging, ex vivo cell marker analysis, colony formation, self-renewal and differentiation assays. For ex vivo studies, adult *Qkf*-GFP SVZ cells were sorted according to their level of GFP expression by FACS. As outlined above, after selecting for single live cells and excluding debris (Fig. 1H), four cell fractions were collected on the basis of their *Qkf*-GFP reporter expression (Fig. 1I).

Subventricular cells with highest *Qkf* expression exhibit the highest capacity for neurosphere colony formation

Cells sorted from adult *Qkf*-GFP SVZ of seven transgenic founder lines were assayed for the formation of colonies of proliferating cells (neurospheres) and showed a strong positive correlation between *Qkf*-GFP expression levels and the ability to form neurospheres (Fig. 2A, data summarized in B; $r=0.7800$, $P<0.0001$, two-tailed test). The *Qkf*-GFP^{Hi} fraction gave rise to the highest number of neurospheres, which was significantly more than the three other fractions ($P<0.0001$, $n=28$ *Qkf*-GFP sorts using one animal each). By contrast, neurospheres were rare in cell fractions with the lowest *Qkf*-GFP expression. A 130-fold

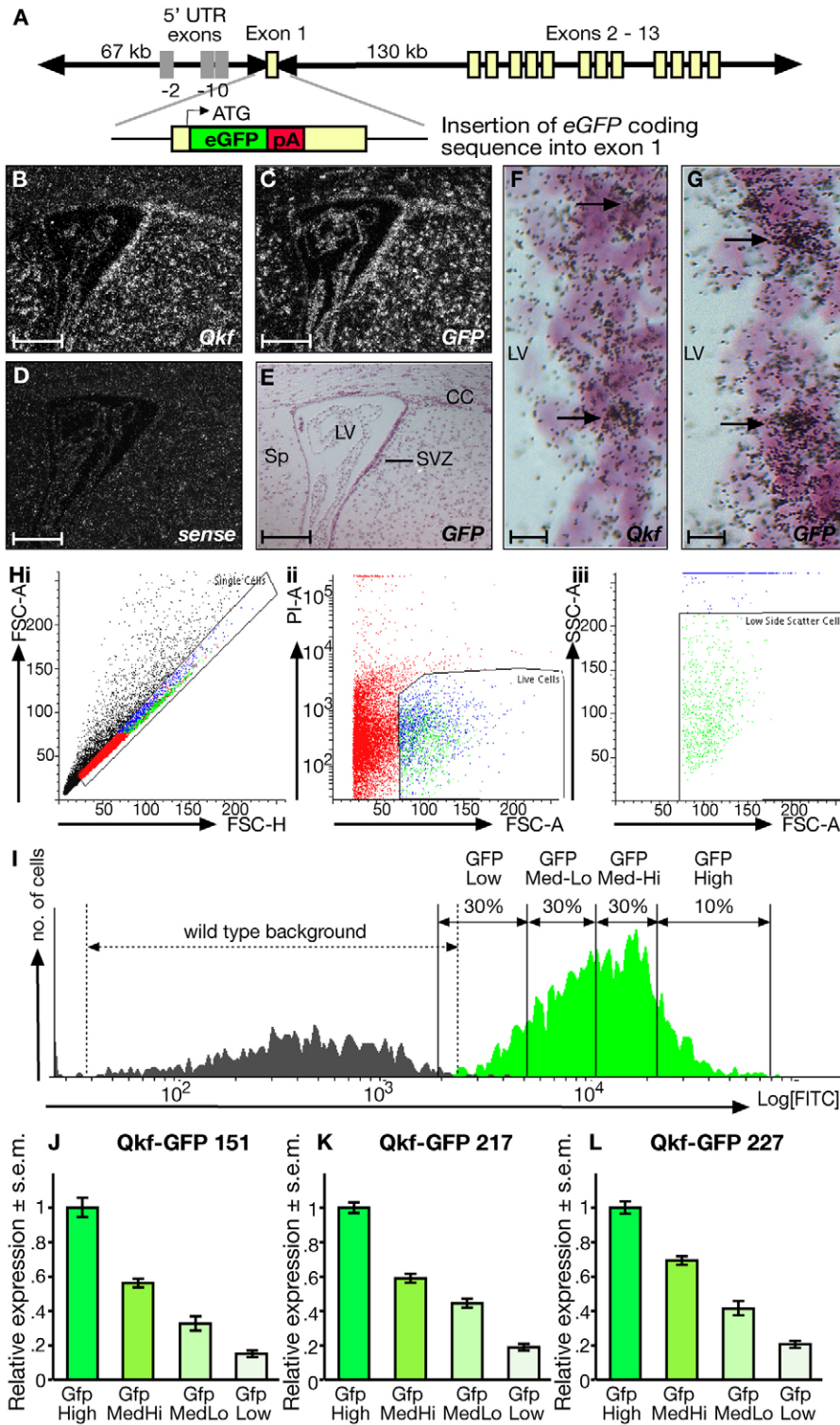


Fig. 1. The *Qkf*-GFP transgenic mouse strains and the SVZ cell sorting strategy. (A) The construct used to generate *Qkf*-GFP transgenic mice contained exons -2 to 13 of the *Qkf* gene and 67 kb of upstream sequence, totalling 197 kb of *Qkf* genomic sequence. The *eGFP* coding sequence was inserted in the first coding exon of the *Qkf* gene on BAC pLD53SCA-E-B. (B-G) In situ hybridization shows the overlap between endogenous *Qkf* and *GFP* transgene expression in the SVZ. *Qkf* probe 1332, which hybridizes to a 1.6 kb fragment of exon 16, not present in the *Qkf*-GFP transgenic vector, shows strong *Qkf* expression in the SVZ (B). The *Qkf*-GFP transgene expression (C, dark-field illumination; E, bright-field illumination) closely resembles endogenous *Qkf* expression in an adjacent slide of the same brain in B. (D) Sense control hybridization. (F,G) High magnification images show strong *Qkf* and *GFP* expression in individual subependymal cells of the SVZ. (H,I) FACS sorting strategy to isolate SVZ cell populations with different levels of *Qkf* promoter activity driving *GFP* expression. (H) Single cells (i) and live cells (ii; propidium iodide negative) were gated. Debris was excluded on the basis of forward scatter and side scatter (FSC-A, SSC-A, iii). Four cell fractions were collected according to their *Qkf*-GFP expression levels (I), and used for subsequent experiments. (J-L) Endogenous *Qkf* expression levels in sorted cell populations. Each graph represents one animal and error bars indicate technical variation. For all data combined (J-L; $n=3$ animals from three independent lines), $P<0.0001$ for all multi-comparisons. CC, corpus callosum; LV, lateral ventricle; Sp, septum; SVZ, subventricular zone. Scale bars: 173 μ m in B-E and 14 μ m in F,G.

enrichment for neurosphere forming cells was observed in the *Qkf*-GFP^{Hi} fraction over the *Qkf*-GFP^{Lo} fraction, a 12-fold enrichment over unsorted cells ($P<0.0001$, $n=28$ *Qkf*-GFP sorts and six unsorted SVZ cultures from one animal each) and a 4.5-fold enrichment over wild-type cells sorted by FACS using the same criteria as those described in Fig. 1H ($P<0.0001$, $n=28$ *Qkf*-GFP sorts, $n=3$ wild-type sorts). Our data suggest that high

Qkf expression correlates with neurogenic activity of SVZ cells. Indeed, the *Qkf*-GFP^{Hi} population was so highly enriched for neurosphere-forming cells that sorting of SVZ cells using a combination of stem cell markers, which individually enrich for neurosphere-forming cells (*Qkf*-GFP^{Hi}, SSEA-1 positive, CD133 positive, HSA^{Lo}), did not result in further enrichment (data not shown).

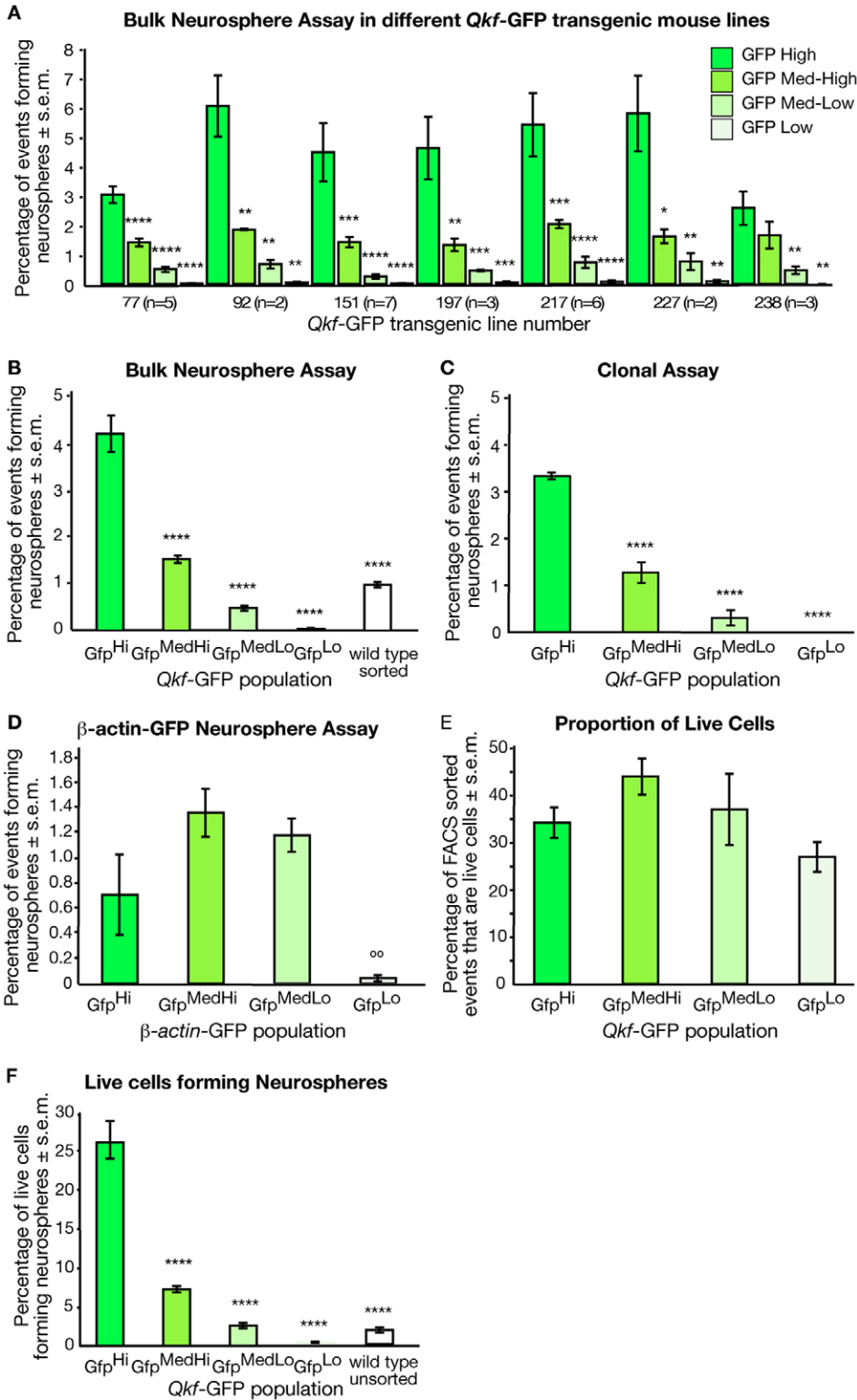


Fig. 2. High *Qkf* promoter activity corresponds to a high capacity to form neurosphere colonies. (A) Neurosphere colony formation in the four cell fractions expressing different levels of *Qkf*-GFP examined in seven independent *Qkf*-GFP transgenic founder mouse lines. (B) Summarized results of all the lines presented in A. (C) Clonal colony-formation assays. Note the strong positive correlation between *Qkf*-GFP expression and colony formation. (D) Control neurosphere colony formation assayed in a mouse line expressing GFP under the control of the β-actin promoter. (E) Cell viability of the enzymatically and mechanically dissociated, and FACS sorted SVZ was on average 35% of all sorted events in the four sorted populations. (F) Proportion of live cells forming neurospheres (on the basis of cell viability data in E and supplementary material Fig. S2). Asterisks indicate a significant difference between the marked fraction and *Qkf*-GFP^{Hi} at **P*<0.05, ***P*<0.01, ****P*<0.001, *****P*<0.0001. Circles in D indicate a significant difference between *Qkf*-GFP^{Lo} and *Qkf*-GFP^{MedHi} or *Qkf*-GFP^{MedLo}; *P*<0.01. See supplementary material Tables S1–S6 for multiple comparisons and exact *P*-values. Data were analyzed as described in the Materials and Methods.

Because plating density can influence the efficiency of neurosphere colony formation (Capela and Temple, 2002), we carried out clonal assays. Cells were sorted as described above, and each sorted event was plated into a well of a 96-well plate. Consistent with bulk culture, a strong, positive correlation between *Qkf*-GFP expression levels and neurosphere forming ability was observed ($r=0.8997$, $P<0.0001$; Fig. 2C). The

number of neurosphere forming cells was significantly higher in the *Qkf*-GFP^{Hi} fraction than in all other fractions ($P<0.0001$, $n=3$). Therefore, plating densities did not affect the relationship between *Qkf*-GFP expression levels and neurosphere formation.

To ensure that GFP expression on its own did not affect colony formation, SVZ cells from β-actin-GFP transgenic mice (Hadjantonakis et al., 1998) were sorted as described in

Fig. 1H,I and assayed for neurosphere colony formation. Although there was some variation in the colony-forming capacity of SVZ cells expressing different levels of β -actin-GFP, this pattern was distinctly different from that observed in Qkf -GFP mice (Fig. 2D compare with B); no significant correlation was found between β -actin-GFP expression and neurosphere formation ($r=0.4532$, $P=0.140$, $n=4$ β -actin-GFP animals). Therefore, the strong relationship between Qkf -GFP expression levels and neurogenic activity is specific to the regulatory elements of the Qkf gene.

One in four live Qkf -GFP^{Hi} subventricular cells give rise to a neurosphere colony

In contrast to sorted blood cells, only a minority of the FACS events derived from the enzymatically and mechanically dissociated SVZ represent live cells. Therefore, we evaluated the relationship between FACS events and the number of viable cells in the different Qkf -GFP fractions immediately after sorting. Approximately 35% of sorted events were found to be live cells (Fig. 2E). The relationship between FACS events and live cells was similar in all Qkf -GFP fractions, except for a slight reduction in the Qkf -GFP^{Lo} fraction (supplementary material Table S5; $n=4$). This suggests that the correlation between Qkf -GFP expression levels and neurosphere formation is not an artefact due to the proportion of live cells in the different Qkf -GFP fractions at the time of plating.

Enrichment in live cells (rather than sorted events) is commonly used as a baseline in other studies (Capela and Temple, 2002; Coskun et al., 2008; Rietze et al., 2001). When based on the number of sorted cells (Fig. 2E) that are alive 2 hours after plating (supplementary material Fig. S2), one in four live cells in the Qkf -GFP^{Hi} fraction give rise to neurospheres (Fig. 2F), compared with 1:50 unsorted live cells ($P<0.0001$, $n=28$ Qkf -GFP sorts, $n=6$ unsorted wild-type cultures), showing the high enrichment of neurosphere-forming cells in the Qkf -GFP^{Hi} fraction.

High Qkf gene activity indicates self-renewal potential

Self-renewal is one of the defining criteria of stem cells. To determine the relationship between Qkf -GFP expression levels and the self-renewal potential of SVZ neurosphere-forming cells, long-term passaging was carried out as an in vitro readout for self-renewal. Freshly isolated SVZ cells were sorted on the basis of Qkf -GFP expression and plated at equal cell densities. After five passages, only the two highest Qkf -GFP-expressing fractions retained proliferating cells (Fig. 3A; $n=6$ Qkf -GFP sorts and cultures). Moreover, two Qkf -GFP^{Hi} and two Qkf -GFP^{MedHi} cultures were chosen and passaged successfully until passage 12. Importantly, there were nearly 15-fold more cells in the Qkf -GFP^{Hi} cultures than in the Qkf -GFP^{MedHi} cultures after five passages, suggesting that a substantial proportion of the Qkf -GFP^{MedHi} colonies were progenitor colonies with limited self-renewal capacity. The two lowest Qkf -GFP fractions did not maintain any self-renewal activity. Even though live cells were present in these fractions at passage one, by the third passage, no proliferating cells were present in the Qkf -GFP^{Lo} culture. Similarly, only one out of six Qkf -GFP^{MedLo} cultures was able to proliferate beyond passage four, and no live cells were present in this culture at passage 6. The strong positive correlation between Qkf -GFP expression and self-renewal ability shows that

high Qkf levels are indicative of the self-renewal potential of NSCs ($r=0.9045$, $P<0.0001$).

Highest Qkf promoter activity indicates the highest proliferative capacity

Neurospheres contain stem cells, transit amplifying cells and lineage-restricted proliferating progeny. In the neurosphere assay, stem cells are thought to have an increased proliferation rate and capacity compared with progenitor cells (Louis et al., 2008; Reynolds and Rietze, 2005). We determined the proliferative capacity of SVZ colony-forming cells by assessing the size of neurospheres in the different Qkf -GFP-expressing fractions.

SVZ cells were sorted on the basis of Qkf -GFP expression and plated in a semi-solid medium containing collagen. Colonies were grown for 3 weeks and then scored. Stem cell colonies are designated as colonies that are larger than 2 mm in diameter three weeks after plating (Fig. 3B). The Qkf -GFP^{Hi} fraction formed the highest proportion of stem cell colonies, more than the Qkf -GFP^{MedHi} in trend fraction ($P=0.092$, $n=7$) and significantly more than the two lowest Qkf -GFP-expressing fractions ($P<0.01$), which very rarely formed large colonies (Fig. 3C). Interestingly, one in 3.5 Qkf -GFP^{Hi} colonies were larger than 2 mm, suggesting that 29% of neurosphere-forming cells in the Qkf -GFP^{Hi} are NSCs. There was a significant, positive correlation between stem cell colony formation and Qkf promoter activity ($r=0.8870$, $P<0.0001$).

To determine the proliferation capacity of SVZ cells in bulk neurosphere cultures, the volume of all individual neurospheres in each of the four Qkf -GFP fractions was determined. There was a positive correlation between Qkf -GFP expression levels and the average volume of neurospheres ($r=0.3434$, $P<0.0001$; Fig. 3D). Neurospheres in the Qkf -GFP^{Hi} fraction were on average, more than twice the size of neurospheres in the two low Qkf -GFP-expressing fractions ($P<0.0001$, $n=583$ Qkf -GFP^{Hi} scored neurospheres, 546 Qkf -GFP^{MedHi}, 233 Qkf -GFP^{MedLo}, 26 Qkf -GFP^{Lo}).

Together, our results show that the cells with the highest Qkf levels have the greatest capacity for neurosphere formation (Fig. 2), long-term self-renewal (Fig. 3A) and a high proliferative capacity (Fig. 3C,D), indicative of stem cell activity. The experiments above indicated that Qkf gene activity traced NSC identity as assessed by ex vivo and in vitro experiments. In the next section, we examined the relationship between Qkf gene activity and NSC identity in vivo.

The slow-cycling neural stem cells have the highest Qkf promoter activity in vivo

The SVZ neurogenic region contains cell types with different cell cycle characteristics. Transit amplifying cells and neuroblasts are thought to divide approximately every 12–18 hours, whereas NSCs divide once every 14–15 days (Craig et al., 1999; Morshead et al., 1998). Cells can be identified by their cell cycle length using both the thymidine analogue BrdU, which is incorporated into cellular DNA during S phase of the cell cycle, and Ki67, which is an endogenous marker for actively proliferating cells in G1, S, G2 or M phase. To mark fast dividing cells (neuroblasts and transit amplifying cells), four BrdU injections were administered over 4 hours, after which the SVZ cells were sorted, spun onto slides and stained for BrdU. Although there was a positive correlation between Qkf promoter activity and the number of short-term BrdU-labelled cells

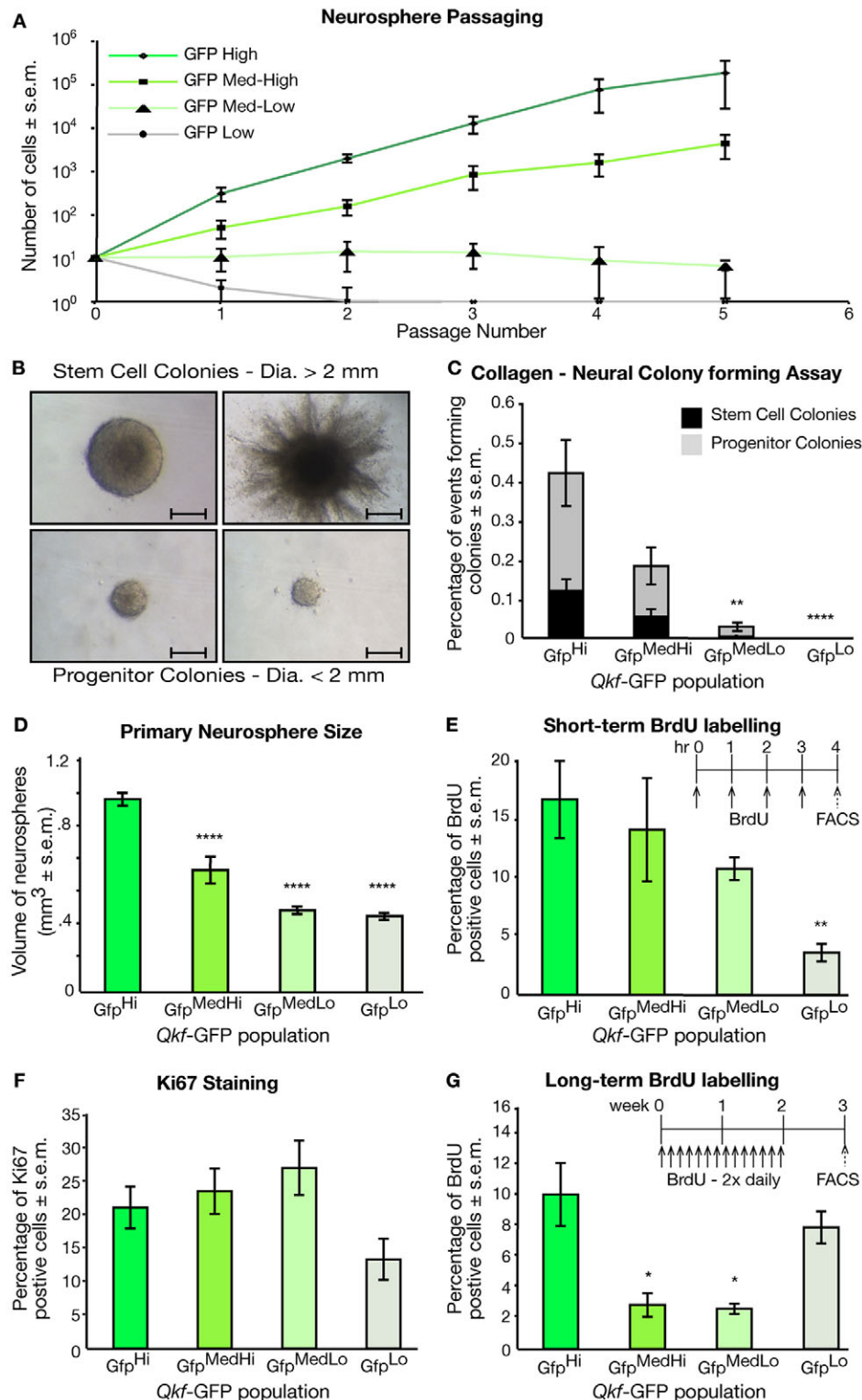


Fig. 3. The highest *Qkf* promoter activity indicates self-renewal, proliferative capacity and cell cycle characteristics of NSCs.

(A) Long-term culture and passing of SVZ neurosphere-forming cells. Note the log scale and that only SVZ cells expressing high levels of *Qkf-GFP* were able to form neurospheres that could be passed and cultured for at least 3 months. (B–D) Proliferative capacity of SVZ colony-forming cells assessed by semi-solid neural colony forming assay (B,C) and measuring the size of neurospheres in bulk suspension cultures (D). (E,F) In vivo assessment of short-term BrdU incorporation by cells (E; four BrdU injections over 4 hours) and Ki67-positive cells (F), corresponding predominantly to transit amplifying cells and neuroblasts. (G) In vivo assessment of long-term BrdU incorporation by cells, corresponding to the slow-cycling NSC and terminally differentiated cells (bi-daily BrdU injections for 14 days, followed by 7 days without treatment before FACS analysis). Asterisks indicate a significant difference between the marked fraction and *Qkf-GFP^{Hi}* at * $P < 0.05$, ** $P < 0.01$, *** $P < 0.001$, **** $P < 0.0001$. See supplementary material Tables S7–S11 for multiple comparisons and exact P -values. Scale bars: 1 mm (B). Data were analyzed as described in the Materials and Methods.

($r = 0.6962$, $P = 0.0027$; Fig. 3E), the number of cells showing short-term incorporation of BrdU was not significantly different between the three strongest *Qkf-GFP*-expressing fractions ($P > 0.15$, $n = 4$). Only the *Qkf-GFP^{Lo}* fraction contained significantly fewer cells in S phase than the *Qkf-GFP^{Hi}* and *Qkf-GFP^{MedHi}* fractions ($P = 0.0066$ and 0.0219). All four

fractions contained comparable numbers of Ki67-positive cycling cells ($P > 0.10$, $n = 3$; Fig. 3F). Therefore, fast-cycling cells are present in all four *Qkf-GFP* fractions.

To assess the number of the infrequently dividing NSCs, we carried out a long-term BrdU incorporation experiment. Mice were injected twice daily with BrdU for 2 weeks, followed by 1

week without treatment. BrdU is distributed to daughter cells through cell division, and thereby becomes more dilute as cells divide. Therefore, any cells positive for BrdU after 1 week without treatment are slow-dividing or terminally differentiated cells. Following the 3-week BrdU labelling procedure, SVZ cells were sorted on the basis of their *Qkf-GFP* reporter expression, and stained for BrdU. Approximately 10% of *Qkf-GFP^{Hi}* cells were positive for BrdU, which was significantly more than in the *Qkf-GFP^{MedHi}* and the *Qkf-GFP^{MedLo}* fraction ($P < 0.05$, $n = 3$; Fig. 3G). Interestingly, 8% of *Qkf-GFP^{Lo}* cells were also positive for BrdU after the 3-week procedure. However, on the basis of the colony-forming and proliferation assays (Figs 2, 3), these cells lacked the ability to give rise to neurosphere colonies or to divide more than five times in vitro. Therefore, it is probable that the long-term BrdU-incorporating cells in the *Qkf-GFP^{Lo}* fraction were terminally differentiated cells. Remarkably, this shows that the level of *Qkf-GFP* expression distinguishes between long-term BrdU-labelling NSCs and terminally differentiated cells. In conclusion, the *Qkf-GFP^{Hi}* fraction contains the great majority of slow dividing, self-renewing, neurosphere colony-forming cells, whereas all four *Qkf-GFP* fractions contain some other type of proliferating cells.

Subventricular cells with the highest *Qkf* promoter activity express neural stem cell markers

NSCs are widely considered to be astrocyte-like cells in the subependymal layer of the SVZ, which express the mature astrocyte marker GFAP (Doetsch et al., 1999; Garcia et al., 2004; Morshead et al., 2003a). In addition, heat stable antigen (HSA, CD24), which is expressed on the surface of ependymal cells and neuroblasts (Calaora et al., 1996), is expressed at low levels in neurosphere-forming cells (Rietze et al., 2001). This is consistent with the observation that NSCs reside in the subependymal layer of the SVZ (Chiasson et al., 1999; Doetsch et al., 1999; Laywell et al., 2000). SSEA-1 has been used for the enrichment of NSCs from the adult SVZ and embryonic brains. Between 12.5% and 25% of sorted SSEA-1-positive cells form neurospheres (Capela and Temple, 2002; Capela and Temple, 2006). In addition to a GFAP-positive NSC population in the subependymal layer, a smaller, more quiescent population of NSCs expressing CD133 has been reported (Coskun et al., 2008; Beckervordersandforth et al., 2010).

To determine the cellular identity of the four *Qkf-GFP* fractions, we examined the expression of specific SVZ cell markers either by flow cytometry or by immunofluorescent staining and counting of acutely sorted SVZ cells. There was a strong positive correlation between *Qkf-GFP* expression and the proportion of GFAP-positive ($r = 0.7818$, $P = 0.0003$, $n = 4$; Fig. 4A), HSA^{Lo} ($r = 0.7964$, $P < 0.0001$, $n = 6$; Fig. 4B), SSEA-1-positive ($r = 0.9079$, $P < 0.0001$, $n = 7$; Fig. 4C) and CD133-positive ($r = 0.7242$, $P = 0.0077$, $n = 3$; Fig. 4D) cells. In particular, 65% of sorted events in the *Qkf-GFP^{Hi}* population were positive for GFAP, which was threefold higher than the *Qkf-GFP^{MedHi}*, and sixfold higher than the *Qkf-GFP^{MedLo}* and *Qkf-GFP^{Lo}* fractions ($P < 0.0001$; Fig. 4A). Similarly, approximately 80% of sorted events in the *Qkf-GFP^{Hi}* and *Qkf-GFP^{MedHi}* fractions expressed HSA at low levels, which was significantly more than the two lowest *Qkf-GFP* fractions ($P < 0.0001$; Fig. 4B). Fifty-five percent of sorted events in the *Qkf-GFP^{Hi}* fraction strongly expressed SSEA-1, which was significantly more than the *Qkf-GFP^{MedHi}*, *Qkf-GFP^{MedLo}* and

Qkf-GFP^{Lo} fractions (Fig. 4C; $P < 0.0001$). We found relatively few CD133-positive cells in the SVZ. However, there was approximately sevenfold enrichment for CD133-positive cells in the *Qkf-GFP^{Hi}* fraction, over the *Qkf-GFP^{MedLo}* ($P = 0.0149$; Fig. 4D) and *Qkf-GFP^{Lo}* ($P = 0.0099$) fractions. This suggests that high *Qkf* promoter activity enriches for all cells expressing NSC markers rather than a specific sub-population of stem cells. Altogether, our cell marker analyses show that the SVZ fraction with the highest *Qkf-GFP* expression is highly enriched for the full range of stem cell markers (GFAP positive, HSA^{Lo}, SSEA-1 positive and CD133 positive).

To determine which fractions are likely to contain neuroblasts, we utilized polysialylated neural cell adhesion molecule (PSA-NCAM), a polysialylated cell surface protein specifically expressed on neuroblasts (Doetsch et al., 1997). The largest proportion of PSA-NCAM-positive cells was found in the *Qkf-GFP^{MedLo}* fraction ($P < 0.005$, $n = 3$; Fig. 4E), suggesting that neuroblasts were highly enriched in this *Qkf-GFP^{MedLo}* population. Interestingly, we observed a high overlap between PSA-NCAM expression levels and nestin staining (Fig. 4F, $n = 3$), an intermediate filament that is widely expressed in the SVZ (Doetsch et al., 1997). Our results suggest that endogenous nestin is most strongly expressed in neuroblasts and weakly in other SVZ cell types.

Ependymal cells are differentiated cells that line the lateral ventricle and provide nutrients for cells within the SVZ NSC niche. While HSA is weakly expressed on the surface of NSCs and progenitor cells, it is strongly expressed on ependymal cells and neuroblasts (Calaora et al., 1996). To determine whether ependymal cells were enriched in any of the *Qkf-GFP* fractions, we screened for the presence of HSA expression, and absence of PSA-NCAM staining in the four *Qkf-GFP* populations (see Fig. 4Bii-v for HSA^{Hi} population and E for PSA-NCAM^{Hi} population). Only 9.8% and 11.5% of *Qkf-GFP^{Hi}* and *Qkf-GFP^{MedHi}* sorted events, respectively, stained strongly for HSA, which was significantly less than the *Qkf-GFP^{MedLo}* (53.6%) and *Qkf-GFP^{Lo}* (65.4%) fractions ($P < 0.0001$, $n = 6$; Fig. 4B). Migrating neuroblasts coexpress HSA and PSA-NCAM (Calaora et al., 1996). Because 43% of the sorted events in the *Qkf-GFP^{MedLo}* fraction were PSA-NCAM positive, it is probable that the majority (43 of 53.6, i.e. 80%) of the HSA-positive cells in this fraction were PSA-NCAM-HSA double positive neuroblasts. By contrast, only a small proportion of FACS sorted events in the *Qkf-GFP^{Lo}* fraction were PSA-NCAM positive (16%), whereas strong HSA staining was common (65.4% of all FACS events). Therefore, HSA-positive, PSA-NCAM-negative ependymal cells are likely to be enriched in the *Qkf-GFP^{Lo}* population.

Altogether, our cell marker analyses suggest that the *Qkf-GFP^{Hi}* fraction contained most of the NSCs, the *Qkf-GFP^{MedHi}* fraction was enriched for transit amplifying cells, and the *Qkf-GFP^{MedLo}* fraction mostly contained neuroblasts, whereas the *Qkf-GFP^{Lo}* population was enriched for ependymal cells.

GFAP-positive subventricular zone stem cells express *Qkf-GFP* at high levels

Our analyses have revealed that the acutely isolated *Qkf-GFP^{Hi}* population was enriched for stem cell markers and was highly enriched for self-renewing neurosphere-colony forming cells. To further investigate the overlap between high *Qkf* expression and

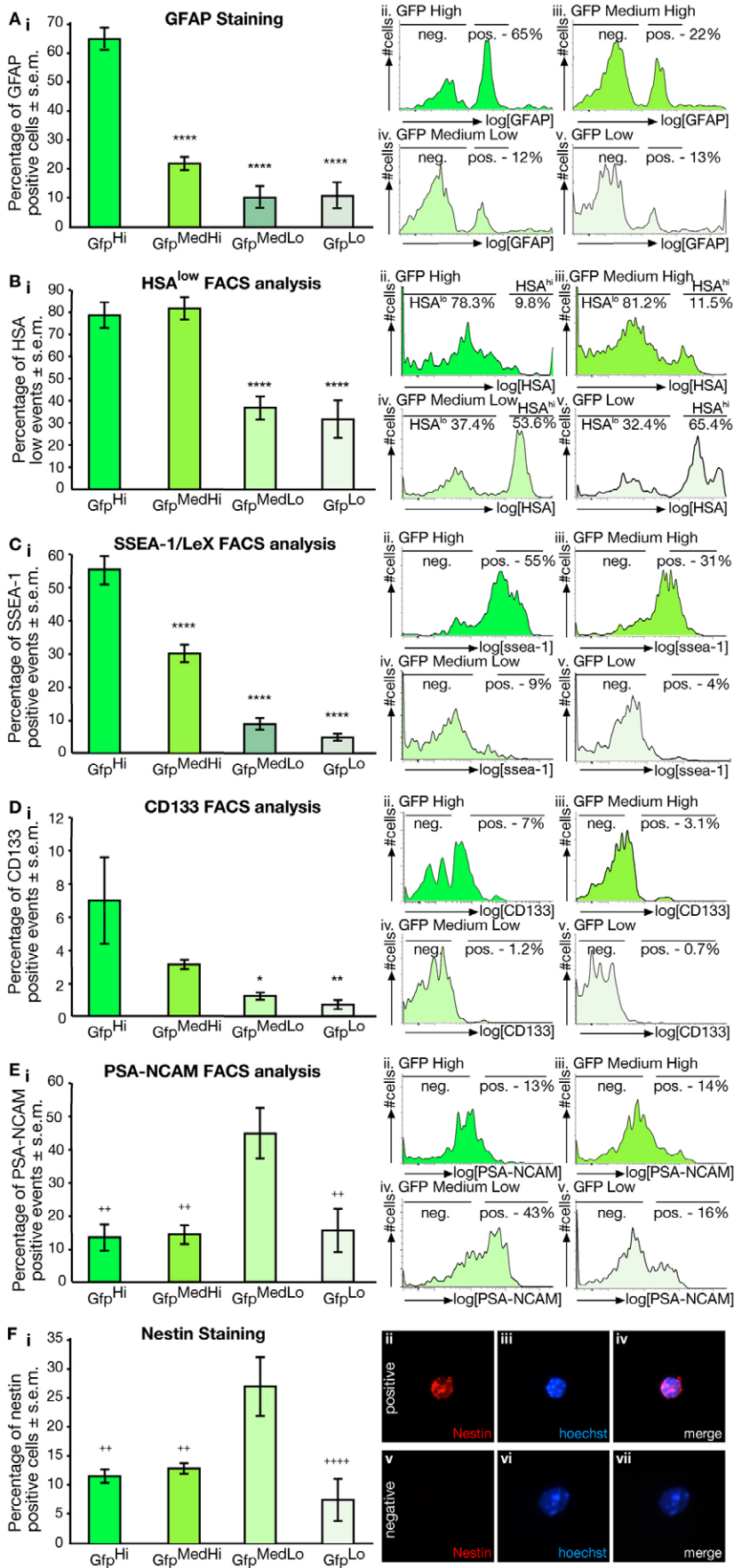


Fig. 4. Cells of the *Qkf-GFP^{Hi}* fraction express known NSC markers. The markers GFAP (A), HSA (B), SSEA-1 (C), CD133 (D) and PSA-NCAM (E) were analyzed by flow cytometry; (i) quantifications and (ii–v) flow cytometry profiles. (F) Nestin (red) immunofluorescence in cells collected by FACS and cytospun; (i) quantifications and (ii–vii) immunofluorescence images. Asterisks indicate a significant difference between the marked fraction and *Qkf-GFP^{Hi}* at * $P < 0.05$, ** $P < 0.01$, *** $P < 0.001$, **** $P < 0.0001$; + symbols in E and F indicate a significant difference between the marked fraction and *Qkf-GFP^{MedLo}* at ++ $P < 0.01$, +++ $P < 0.001$, ++++ $P < 0.0001$. See supplementary material Tables S12–S17 for multiple comparisons and exact P -values. Data were analyzed as described in the Materials and Methods.

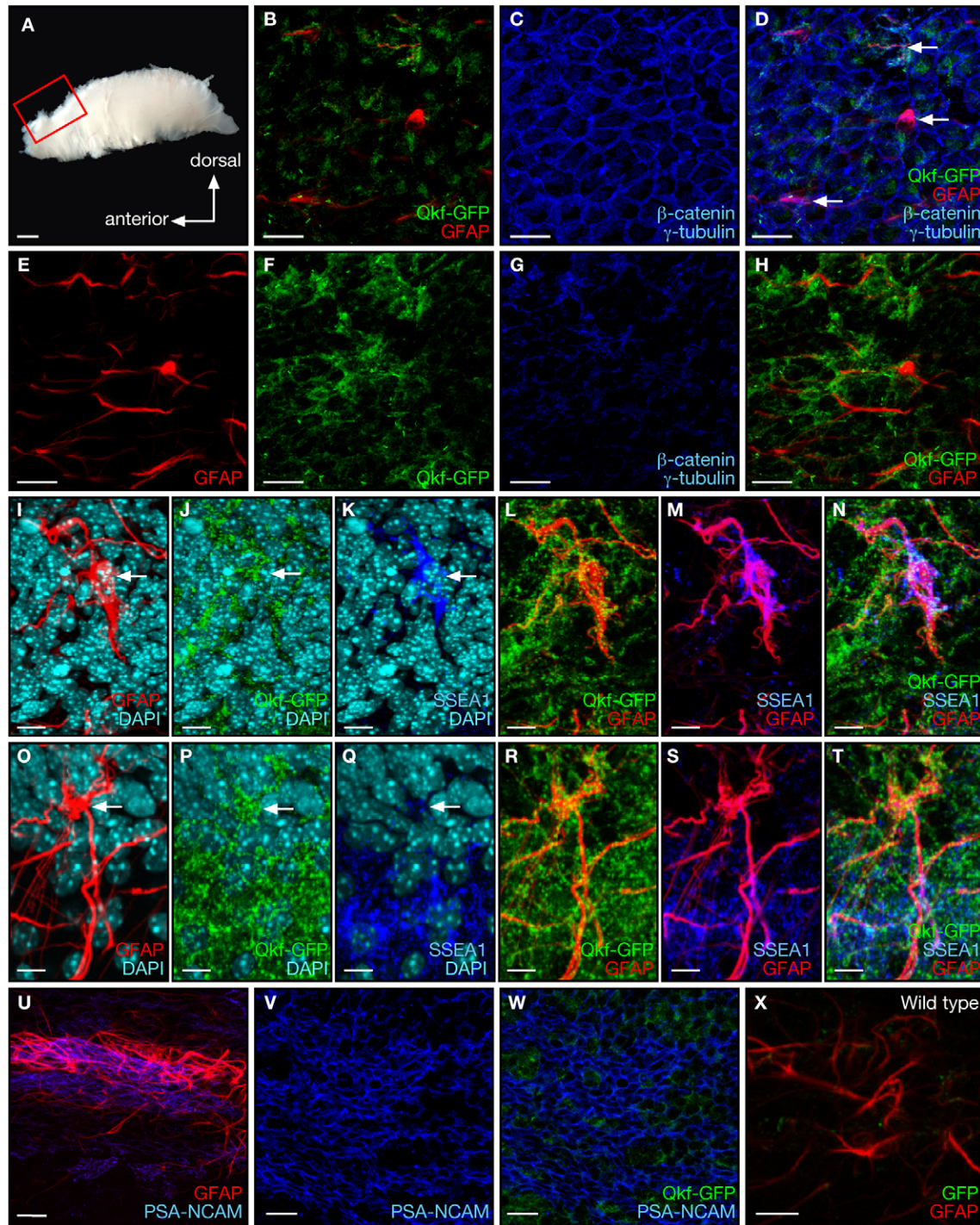


Fig. 5. GFAP-positive stem cells overlap with strong *Qkf-GFP* expression in vivo. (A) All confocal images were taken in the anterior–dorsal SVZ region of the lateral wall of the lateral ventricle. (B–D) The honeycomb architecture of the ependymal layer stained with β -catenin and γ -tubulin (both blue) shows little GFAP and *Qkf-GFP* staining. Some GFAP-positive processes are intercalated in the ependymal layer (red; arrows in D). (E–H) Immediately below the ependymal layer GFAP-positive processes are evident. (I–T) In the subependymal layer, cell bodies of GFAP-positive cells (I, O – cell bodies indicated with arrow) co-express *Qkf-GFP* and SSEA-1 (L–N and R–T). (U) Overview of PSA-NCAM-positive neuroblast chains surrounded by GFAP-positive processes of NSCs. (V–W) PSA-NCAM-positive neuroblasts shows little overlap with strong *Qkf-GFP* expression. (X) Wild-type control showing absence of *Qkf-GFP* expression, and the presence of GFAP-positive cells in the SVZ. Scale bars: 500 μ m (A), 20 μ m (B–H), 10 μ m (I–T), 50 μ m (Q), 30 μ m (V–W) and 20 μ m (X).

cell identity in vivo, whole-mount staining of SVZ tissue dissected from *Qkf-GFP* animals was carried out ($n=16$ animals) as described previously (Mirzadeh et al., 2010; Shen

et al., 2008). The results are shown in Fig. 5A and all images depict the anterior–dorsal SVZ in the lateral wall of the lateral ventricle. The ependymal surface of the SVZ was marked using a

combination of β -catenin and γ -tubulin as previously described (Mirzadeh et al., 2008). The typical honeycomb architecture of the ependymal surface was observed. A small number of GFAP-positive stem cell processes were intercalated in the ependymal layer (Fig. 5D, arrows). Consistent with cell surface marker studies, there was very little *Qkf*-GFP expression in the ependymal layer (Fig. 5D). Immediately below the ependymal layer, more GFAP-positive cell processes and a small number of cell bodies were evident (Fig. 5E–H). Sparse *Qkf*-GFP expression was found to overlap with cell bodies of GFAP-positive cells. Deeper in the subependymal layer (Fig. 5I–T), strong overlap was observed between GFAP-positive stem cells and strong *Qkf*-GFP-expressing cells (Fig. 5I,J,L,O,P,R). Analysis of ten high-magnification confocal images taken in the anterior-dorsal region of the SVZ (Fig. 5A) across four different animals revealed that 88% of GFAP-positive cells in the subependymal zone (i.e. 44 out of 50) overlapped with strong *Qkf*-GFP expression (e.g. Fig. 5L,R). This is consistent with flow cytometry data, which showed that 87% of GFAP-positive SVZ cells are found in the *Qkf*-GFP^{Hi} and *Qkf*-GFP^{MedHi} populations. Similarly, strong SSEA-1 expression was found in 66% (42 out of 64) of GFAP-positive cells (Fig. 5I,K,M,O,Q,S). Remarkably, 94% ($n=35$) of cells that were double positive for SSEA-1 and GFAP were found to express *Qkf*-GFP strongly (Fig. 5N). This overlap between strong *Qkf*-GFP, GFAP and SSEA-1 expression was unique, because GFAP and strong *Qkf*-GFP expression was not found in ependymal cells (Fig. 5B–D) or in PSA-NCAM-positive neuroblasts (Fig. 5U–W). Together, these data reiterate that strong *Qkf* expression was largely confined to GFAP- and SSEA-1-double-positive stem cells.

Subventricular cells with high *Qkf* gene activity are multipotent

Another defining criterion for stem cells is multipotency, i.e. the ability to give rise to a range of progeny. When induced to differentiate, NSCs give rise to all three major neural cell types, namely neurons, astrocytes and oligodendrocytes. To elucidate the correlation between *Qkf*-GFP transgene expression and multipotency, SVZ cells were sorted and collected on the basis of their levels of *Qkf*-GFP expression, grown as neurospheres for 7 days and then allowed to differentiate for 7 days before staining for markers of neurons (β III-tubulin), oligodendrocytes (O4) and astrocytes (GFAP). At total of 25 to 30 neurospheres were differentiated from each *Qkf*-GFP fraction from each mouse (SVZ cells were sorted from $n=3$ animals). The exception was the *Qkf*-GFP^{Lo} fraction, as it rarely gave rise to neurospheres.

Only the *Qkf*-GFP^{Hi} and *Qkf*-GFP^{MedHi} fractions generated all three neuronal cell types (Fig. 6A–H). *Qkf*-GFP^{MedLo} neurospheres failed to give rise to oligodendrocytes (Fig. 6I–L), and the *Qkf*-GFP^{Lo} neurospheres only formed astrocytes (Fig. 6M–P). To determine the proportion of *Qkf*-GFP^{Hi} and *Qkf*-GFP^{MedHi} colonies that were multipotent, individual neurosphere colonies were randomly picked and differentiated separately. Twenty-five of forty-two (60%) *Qkf*-GFP^{Hi} colonies ($n=6$ animals) were found to be tripotent, eight (19%) were bipotent and nine (21%) only formed astrocytes. This is significantly more than the number of *Qkf*-GFP^{MedHi} colonies (six out of eighteen, i.e. 33%; $P=0.011$) that were tripotent. Three out of eighteen (17%) *Qkf*-GFP^{MedHi} colonies were bipotent, and nine out of eighteen (50%) colonies only formed astrocytes. In short, the majority of *Qkf*-GFP^{Hi}-derived

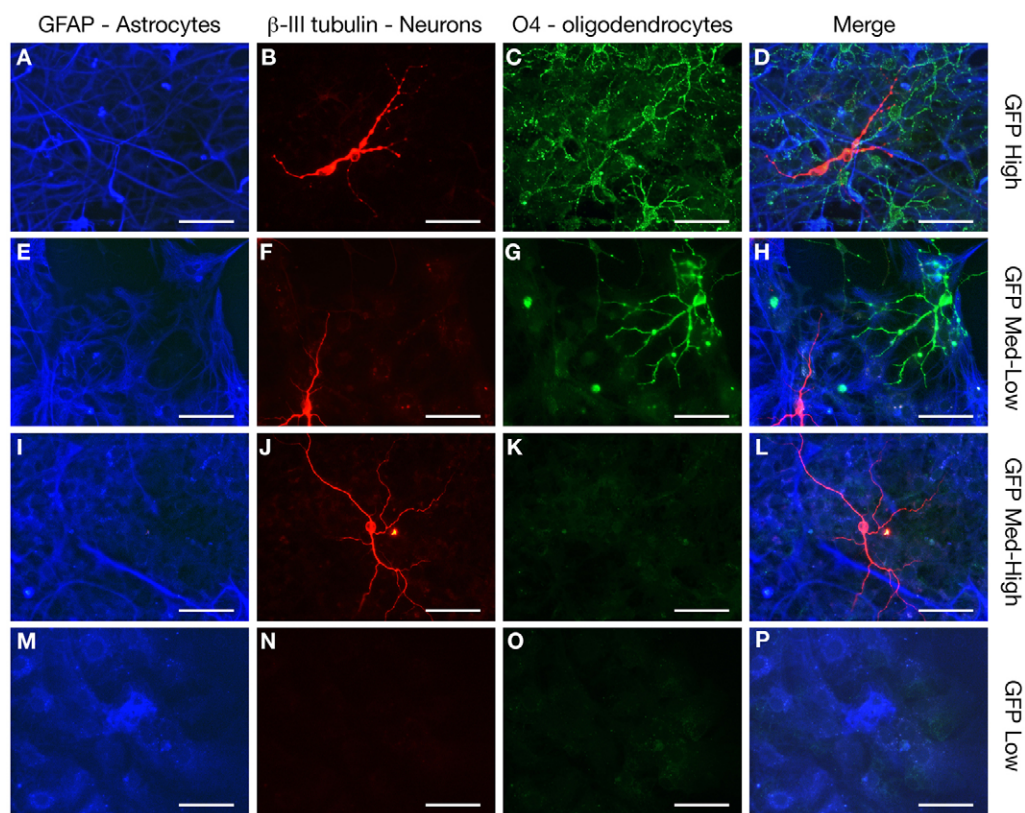


Fig. 6. High *Qkf* promoter activity indicates multipotency. (A–P) Sorted SVZ cells cultured as neurospheres for 7 days, then differentiated on a laminin substrate and stained for markers of astrocytes (GFAP, blue), neurons (β III-tubulin, red) and oligodendrocytes (O4, green). Note that only the two strongest *Qkf*-GFP-expressing fractions were able to produce all three differentiated progeny (A–H). *Qkf*-GFP^{MedLo} neurospheres were unable to form oligodendrocytes (I–L), and *Qkf*-GFP^{Lo} neurospheres were only able to differentiate into astrocytes (M–P). Scale bars: 50 μ m.

neurospheres were tripotent, whereas the majority of *Qkf-GFP^{MedH1}*-derived neurospheres were not tripotent. These data suggest that multipotency, as determined using the neurosphere assay, is correlated with high *Qkf-GFP* expression and thus *Qkf* serves as a marker for multipotent SVZ cells.

Bmi1 mutant mice show an age-dependent decrease in *Qkf-GFP* expression

Bmi1, a member of the polycomb group repressive complex, is important for maintaining self-renewing NSCs through inhibition of the *Ink4a* and *Arf* locus (Molofsky et al., 2003). Owing to a self-renewal defect, the number of NSCs decreases in *Bmi1*^{-/-} mice in an age-dependent manner. When *Qkf-GFP* cell populations were analysed in *Bmi1* mutant and wild-type littermates, a reduction in the *Qkf-GFP^{Hi}* population was observed in the *Bmi1*^{-/-} mice, which declined considerably with age (Fig. 7). This suggests that high *Qkf-GFP* levels, which mark self-renewing multipotent NSCs, accurately report the time-dependent decrease in NSCs previously described in *Bmi1* knockout mice.

Discussion

In this study, we have utilized *Qkf-GFP* BAC transgenic mice to examine the expression levels of *Qkf* in the adult SVZ NSC niche, with respect to stem cell characteristics (summarized in Fig. 8 and supplementary material Table S18).

The definition of a stem cell, as coined by Potten (Potten and Loeffler, 1990), designates stem cells as being (a) undifferentiated, (b) proliferative, (c) self-maintaining (i.e. self-renewing) and (d) able to give rise to a range of functional progeny (i.e. multipotent). Utilizing the neurosphere assay, widely used and accepted as a good test of NSC characteristics (Capela and Temple, 2002; Doetsch et al., 1999; Jensen and Parmar, 2006; Morshead et al., 2003b; Reynolds and Weiss, 1992), we have shown that undifferentiated, proliferative, self-renewing and multipotent cells are largely confined to

approximately the 1000–1500 strongest *Qkf*-expressing cells in the SVZ. In addition, we utilized flow cytometry and confocal microscopy of SVZ whole mounts, to demonstrate that the *Qkf-GFP^{Hi}* fraction was highly enriched for the reported stem cell markers GFAP^{Pos}, HSA^{Lo}, SSEA-1^{Pos} and CD133^{Pos}, and not for markers of ependymal cells or neuroblasts (Capela and Temple, 2002; Coskun et al., 2008; Beckervordersandforth et al., 2010; Garcia et al., 2004; Mirzadeh et al., 2008; Morshead et al., 2003a; Rietze et al., 2001; Shen et al., 2008). Exploiting *Bmi1* mutant mice, which have a severe defect in NSC self-renewal (Molofsky et al., 2003), we have shown that there is an age-dependent decline in the *Qkf-GFP^{Hi}* population in the *Bmi1*^{-/-} mutant mice. Consistent with our conclusion that adult NSCs have the highest requirements for *Qkf* expression, we have previously shown that QKF is required for normal numbers of adult NSCs (Merson et al., 2006; Rietze et al., 2001), and is essential to promote NSC self-renewal and neuronal differentiation (Merson et al., 2006). We have shown that high level *Qkf* expression is restricted to the NSCs (and not their cellular neighbours) and that a high-level *Qkf* expression is essential for long-term self-renewal and multipotency. NSCs are greatly reduced in number in vivo and ex vivo in QKF-deficient animals. Importantly, NSC capacity, which is confined to the strongest QKF-expressing cells, as outlined in this study, declines with age in QKF-deficient animals relative to wild-type controls, consistent with a progressive self-renewal defect in *Qkf* mutant animals (Merson et al., 2006). Furthermore, neurospheres generated from QKF-deficient animals form fewer neurons than wild-type littermates (Merson et al., 2006), reflecting the lack of neuron production found in *Qkf-GFP^{Lo}* neurospheres in the current study. Accordingly, our data suggest that high *Qkf* promoter activity within NSCs is required to maintain the essential stem cell characteristics of self-renewal and multipotency.

In addition to all NSC characteristics and markers being confined to the strongest *Qkf*-expressing cells, our data showed a remarkable relationship between *Qkf*-promoter activity and cell

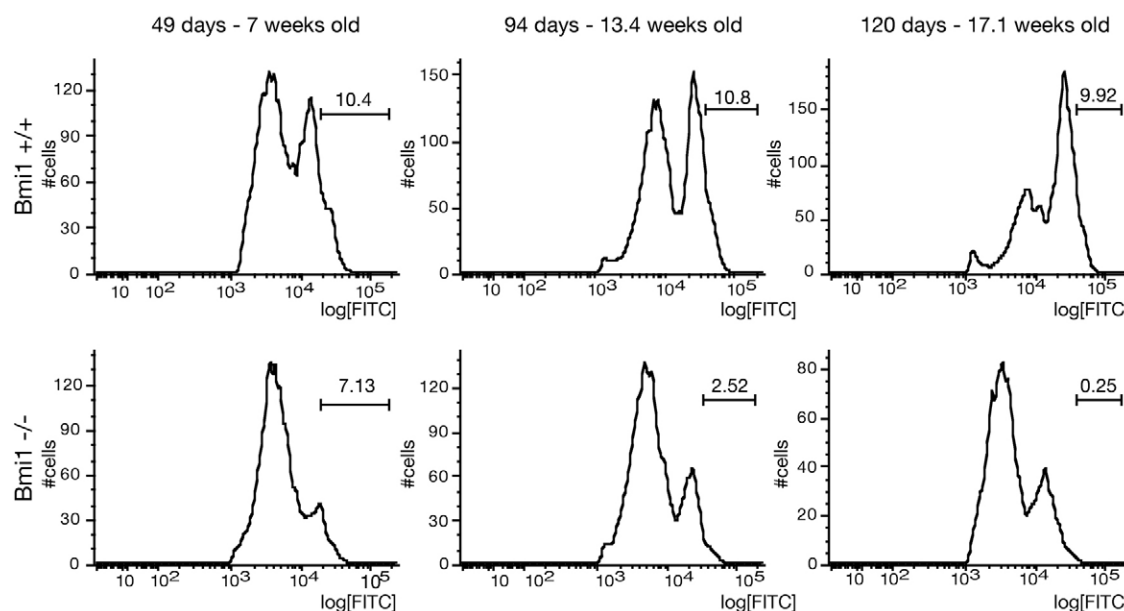


Fig. 7. High *Qkf-GFP* expression decreases in a time-dependent manner on a *Bmi1*-null background. Wild-type littermate controls and *Bmi1* mutants, which show an age-dependent progressive decrease in the *Qkf-GFP^{Hi}* population.

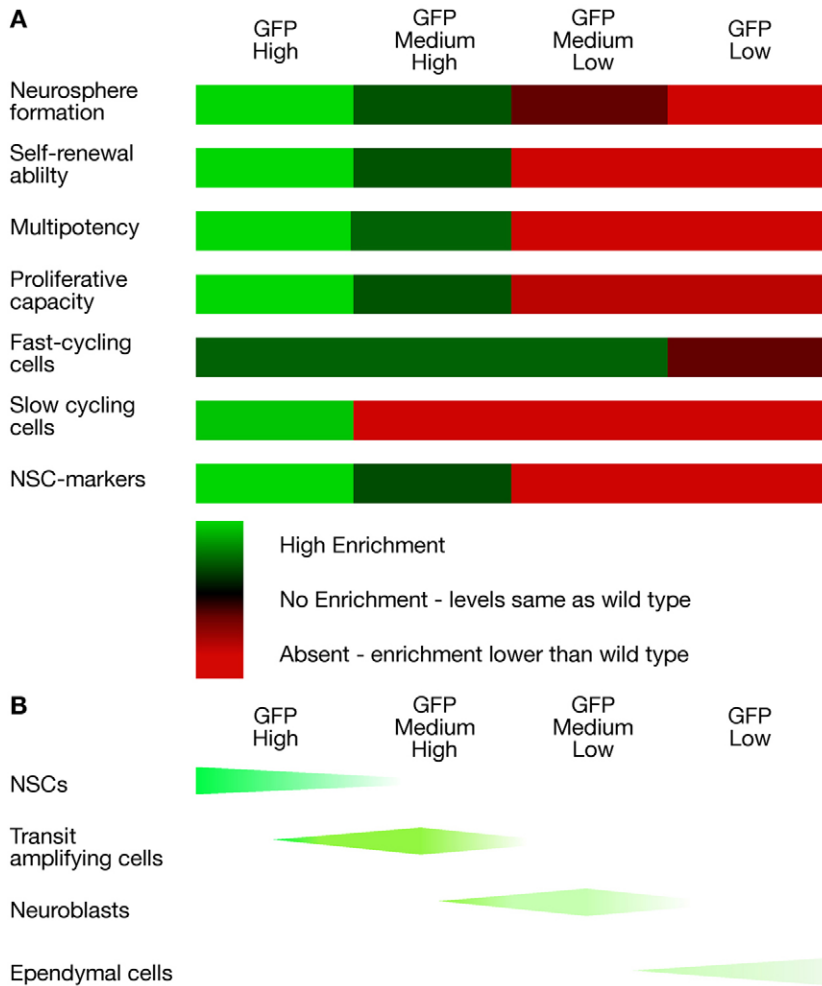


Fig. 8. Schematic summary and interpretation. The central NSC characteristics of neurosphere colony formation, self-renewal ability, multipotency and proliferative capacity strongly correlate with high *Qkf* promoter activity. Together with cell cycle and cell marker analysis, our data suggest that NSCs are highly enriched in the *Qkf*-GFP^{Hi} fraction, transit amplifying cells in the *Qkf*-GFP^{MedHi} fraction, neuroblasts in the *Qkf*-GFP^{MedLo} fraction, and ependymal cells in the lowest *Qkf*-GFP^{Lo} fraction.

identity within the NSC niche. Although our data suggest that there are also a number of stem cells in the *Qkf*-GFP^{MedHi} population, there was enrichment for colony-forming cells with limited self-renewal and proliferative capacity, suggesting that transit amplifying cells are enriched in this *Qkf*-GFP^{MedHi} fraction. Until recently, transit amplifying cells have been difficult to isolate and distinguish from NSCs using cell surface markers. Utilizing *GFAP*-GFP mice, Pastrana and co-workers showed that SVZ cells positive for epidermal growth factor (EGF) receptor, negative for HSA (CD24), with low-level expression of *GFAP* have transit amplifying cell characteristics (Pastrana et al., 2009). Remarkably, we also obtain a high degree of enrichment of transit amplifying cells solely on the basis of medium-high expression of *Qkf*. Interestingly, nearly half of the sorted cells in the *Qkf*-GFP^{MedLo} fraction were PSA-NCAM positive, which is a marker for neuroblasts (Doetsch et al., 1997). These cells are proliferating, lineage-restricted neural precursors with limited proliferative capacity that migrate from the SVZ to the olfactory bulbs (Doetsch and Alvarez-Buylla, 1996). Our data show that this *Qkf*-GFP^{MedLo} fraction also contains the highest percentage of nestin and PSA-NCAM-positive cells, suggesting that migrating, proliferating neuroblasts are enriched in the nestin-positive fraction. While other reports suggest that migrating neuroblasts are indeed nestin positive (Doetsch et al., 1997), NSCs have also been identified as nestin-expressing cells (Reynolds and Weiss, 1992), and various astrocyte

subpopulations are reported to express nestin at the highest level within the SVZ neurogenic region (Doetsch et al., 1997). Together with the current study, these data suggest that endogenous nestin is not a unique marker for any specific SVZ subpopulation. Lastly, HSA-positive, PSA-NCAM-negative cells were highly enriched in the *Qkf*-GFP^{Lo} fraction and they are likely to represent the ependymal cell population, which has been reported to be PSA-NCAM negative and HSA high (Calaora et al., 1996). Our data document a unique, proportional relationship between *Qkf* expression levels and cell identity in the SVZ, where the strongest *Qkf*-expressing cells show all stem cell characteristics, which are gradually lost along with decreasing *Qkf* promoter activity. Together with our previous reports on the deficiencies in NSC establishment and self-renewal in the *Qkf*-deficient state, we suggest that *Qkf* serves both as a NSC intrinsic regulator and as a marker of 'stemness' – the self-renewal potential and multipotency of SVZ cells.

Interestingly, when *Qkf*-GFP expression was assayed in a *Bmi1*-null background, a significant decrease in the *Qkf*-GFP^{Hi} population was observed. Self-renewing multipotent NSCs decrease in an age-dependent manner in *Bmi1* mutant mice because of defects in self-renewal (Molofsky et al., 2003). Given that the *Qkf*-GFP^{Hi} population decreased in *Bmi1* mutant mice compared with littermate controls as mice aged, this finding supports our hypothesis that *Qkf*-GFP expression marks and positively correlates with self-renewing and multipotent SVZ

cells. In addition, this experiment suggests that *Qkf-GFP* transgenic mice can be used to screen a large number of mice for potential defects in NSC self-renewal or multipotency in vivo.

QKF is part of the MYST family of histone acetyltransferases. These epigenetic regulators have an essential function in the control of gene expression through their ability to acetylate histones and modify chromatin structure (Thomas and Voss, 2007; Wang et al., 2009). QKF has an identical domain structure to monocytic leukaemia zinc finger protein (MOZ), and all protein domains are highly conserved between these two transcriptional regulators (Voss and Thomas, 2009). Furthermore, the amino acid sequence within the domains is highly similar. We and others have shown that MOZ has an essential function in the maintenance of haematopoietic stem cells (Katsumoto et al., 2006; Thomas et al., 2006). More recently, it has been shown that the role of MOZ in haematopoietic stem cells is dependent on its histone acetyltransferase activity (Perez-Campo et al., 2009), directly demonstrating the importance of chromatin regulation by this subclass of histone acetyltransferases in stem cells. MOZ was originally identified in recurrent translocations leading to acute myeloid leukaemia (Borrow et al., 1996). Several different chromosomal translocations causing leukaemia target the *MOZ* gene (Aguir et al., 1997; Carapeti et al., 1998; Chaffanet et al., 2000; Chaffanet et al., 1999; Esteyries et al., 2008; Imamura et al., 2003; Kitabayashi et al., 2001; Rozman et al., 2004), and indeed, translocations targeting the human homologue of *Qkf* (*MYST4/KAT6b*) also cause leukaemia (Panagopoulos et al., 2001; Vizmanos et al., 2003). By contrast, deficiency in QKF (*MYST4/MORF*) leads to intellectual disability in humans (Kraft et al., 2011) and brain developmental defects in mice (Thomas et al., 2000). Taken together, these studies show that QKF is a potent regulator of stem-cell characteristics, where loss of function causes brain developmental defects, and gain of function causes malignancy.

Although we are only beginning to understand the role of chromatin structure in establishing and maintaining stem cells, recent studies have demonstrated that stem cell chromatin is unique and actively modified as stem cells differentiate (Bernstein et al., 2006; Mikkelsen et al., 2007). The role of histone acetylation has been studied in embryonic stem cells. Recently, Ware and co-workers have shown that the histone deacetylase inhibitor sodium butyrate was able to maintain self-renewing mouse and human embryonic stem cells without feeder layers or exogenous factors, highlighting the importance of histone acetylation in maintaining a stem cell state (Ware et al., 2009). Interestingly, we have recently shown that the QKF-related protein MOZ is a key regulator of *Hox* gene expression in vivo. MOZ is required to maintain the correct levels of histone 3 lysine 9 (H3K9) acetylation at *Hox* loci during development, and a reduction in MOZ levels leads to aberrant and reduced *Hox* gene expression and an extensive anterior homeotic transformation of the nervous system and the axial skeleton (Voss et al., 2009). The role of H3K9 acetylation in maintaining chromatin structure extends to NSCs. When oligodendrocyte precursors were redirected to become NSC-like self-renewing multipotent cells, the methylated H3K9 was converted to acetylated H3K9 at the promoter of *Sox2* (Kondo and Raff, 2004), a gene essential for maintaining NSCs (Graham et al., 2003). Our data presented here, together with our previous results showing that *Qkf* mutant mice have severe and progressive

defects in adult neurogenesis, suggests that QKF plays a central role in regulating histone acetylation at important stem cell loci within SVZ NSCs.

In conclusion, we have shown that it is possible to isolate the four major populations of the SVZ neurogenic zone, i.e. NSCs, transit amplifying cells, neuroblasts and ependymal cells, on the basis of *Qkf* promoter activity levels. This system will allow the characterization of neural lineage characteristics including the epigenetic mechanisms that regulate NSC self-renewal and lineage commitment in adult neurogenesis.

Materials and Methods

Generation of *Qkf-GFP* transgenic mice

The *Qkf-GFP* BAC construct used for the generation of transgenic mice was generated by homologous recombination in *Escherichia coli* using the method described by Gong et al. (Gong et al., 2002). The *eGFP* coding sequence with its Kozak sequence and poly adenylation signal from *pLD53SCA-E-B* (a gift from Nathaniel Heintz, Rockefeller University, New York, USA) were inserted into the first coding exon of the *Qkf* gene on BAC clone *RP23-121015* replacing the *Qkf* Kozak sequence and start codon. Experiments were performed on male mice aged between 7 and 12 weeks, and conformed to the regulations set by the Australian NHMRC and the Royal Melbourne Hospital Research Foundation. Transgenic mouse lines were maintained as heterozygous for the *Qkf-GFP* transgene and genotyped by the presence of GFP expression in tail biopsies.

Northern Blot analysis, in situ hybridization and RT-qPCR

In situ hybridization was carried out with ³⁵S-labelled dCTP (Amersham) using a method described previously (Thomas et al., 2000). Northern blot analysis was performed using standard molecular biology techniques. *Qkf* probe no. 19 hybridizes to bases 41–1246 of sequence GenBank accession number AF222800, *Qkf* probe no. 1332 to bases 4019–5633 of AF222800, and the *GFP* probe to bases 613–1276 of sequence U55763. To determine endogenous *Qkf* levels in sorted populations, oligonucleotides forward (F) 5'-GCGAATCTCTATGGGTAACG-3' and reverse (R) 5'-GCACTGCTTCAAGATCCAC-3' amplifying from the 5'UTR to exon 1 were used. Expression levels were standardized to 18S (F5'-TCGGAACCTGAGGCCATGATT-3', R5'-CTCCGACTTTCGTTCTTGATT-3'), *Hsp90ab1* (F5'-CCTCCGACTTTCGTTCTTGATT-3', R5'-AGAATCCGACACCAAATGCG-3') and *Gapdh* (F5'-TTCACCACCATGGAGAAGGC-3', R5'-CCCTTTGGCTCCACCCT-3').

FACS and neurosphere culture

SVZ from *Qkf-GFP* transgenic mice were dissected and enzymatically dissociated using pancreatin–trypsin (2.5% pancreatin, 0.5% trypsin). The tissue was mechanically dissociated using a P200 Gilson pipette. Cells were immediately washed in 0.2% BSA in mouse tonicity (MT)-PBS, passed through a 40 µm sieve (Falcon) and collected by centrifugation. Cells were resuspended in 200–300 µl 0.2% BSA in MT-PBS containing 1 µg/ml propidium iodide (Sigma P-4170) to label dead cells. Cells were sorted into four fractions on the basis of their GFP reporter expression using the FACS DiVa (BD Biosciences) and collected in 2 ml 0.2% BSA in MT-PBS. After collection by brief centrifugation, cells from each of the four *Qkf-GFP* fractions were suspended in 5 ml NSC proliferation medium [medium described previously (Merson et al., 2006; Voss et al., 2006)] in a 3.5 cm dish. Neurospheres were counted 3–4 days after sorting. For clonal assays, cells were sorted at a density of one event per well of a 96-well plate containing 150 µl NSC proliferation medium, and counted 7 days after plating.

For passaging, neurospheres were collected by brief centrifugation (7 minutes, 120 g), dissociated mechanically using a P1000 Gilson pipette in approximately 900 µl fresh proliferation medium. Dissociated cells were counted using a haemocytometer and plated at a density of 15,000–30,000 cells per cm² depending on the number of cells available, as described previously (Merson et al., 2006; Voss et al., 2006).

To determine lineage potential, *Qkf-GFP* SVZ cells were sorted and cultured as neurospheres for 7 days. After 1 week in culture, 25–30 neurospheres from each *Qkf-GFP* fraction were induced to differentiate on laminin-treated coverslips in differentiation medium as previously described (Merson et al., 2006). To determine the lineage potential of individual neurospheres, colonies were picked and plated individually in a 24-well plate. Neurosphere cells were allowed to differentiate for 1 week, washed, fixed in 4% paraformaldehyde, blocked in 10% normal goat serum, and stained for astrocytes (GFAP; Dako Z0334; 1:500), oligodendrocytes (O4; MAB345; 1:500) and neurons (βIII-tubulin; Promega G7121; 1:2000).

For cell surface marker analysis, SVZ cells were prepared for flow cytometry and stained with antibodies raised against GFAP (Chemicon MAB3402; 1:500), HSA (mCD24-PE conjugated; Vector B-1075; 1:200), SSEA-1 (BD Biosciences no. 347420; 1:20), CD133 (APC conjugated; eBioscience no. 17-1331-81; 1:1000)

and PSA-NCAM (AbCys AbC0019; 1:400). Alexa Fluor 633 and APC-conjugated anti-mouse IgM and IgG antibodies were used where required. Cells were sorted on the FACS LSR II (BD Biosciences). Sorts were analyzed using FlowJo v8.7 software.

Immunohistochemistry

Whole-mount SVZ staining was carried out as described previously (Mirzadeh et al., 2010). Briefly, *Qkf-GFP* animals were perfusion fixed. The SVZ was dissected and fixed overnight at 4°C in 4% paraformaldehyde. After washing and blocking, the SVZ was incubated with primary antibodies against GFP [using an antibody that was conjugated to biotin (Invitrogen A10263)], GFAP, SSEA-1, PSA-NCAM, β -catenin (Sigma-Aldrich C2206; 1:1000) and γ -tubulin (Sigma-Aldrich T5192; 1:1000) for 48 hours at 4°C. After washing, Alexa Fluor secondary antibodies raised against mouse IgG, IgM and rabbit IgG (Invitrogen Alexa Fluor 633 goat anti-mouse IgG A21052; Alexa Fluor 546 goat anti-rabbit IgG A11035; Alexa Fluor 546 goat anti-mouse IgM A21045; used at 1:500) and FITC-streptavidin (Invitrogen SA1001; 1:500) were applied for 48 hours. Samples were washed, mounted and imaged on the Leica SP2 laser scanning microscope system. Images were processed using the IMARIS v7.2 software.

For BrdU (BioScience Products 010198; 1:10), Ki67 (Novocastra NCL-Ki67p; 1:400) and nestin (Chemicon MAB353; 1:200) staining of SVZ cells collected by FACS, cells were cytopun onto gelatine-coated slides and immunostained as described previously (Voss et al., 2006). Cells were counted and photographed using a compound microscope (Axioplan 2, Zeiss).

Cell viability assays

Cells were collected by centrifugation and suspended in 40 μ l 0.2% BSA in MT-PBS. Trypan Blue (10 μ l, Sigma) was added, mixed, and 10 μ l of the cell suspension was added to each of four areas of a haemocytometer and counted.

Neurosphere proliferation assays

SVZ cells from *Qkf-GFP* animals were sorted as described above. For the neural colony-forming cell assay, cells were suspended in collagen and grown according to manufacturer's instructions (Stemcell Technologies, Vancouver, Canada). Colonies were scored 3 weeks after plating. To determine neurosphere size in bulk cultures, neurospheres were grown for 4 days, after which the size of each neurosphere in each of the *Qkf-GFP* fractions was determined using a scale in the eyepiece of an inverted microscope (10 \times objective, 10 \times magnification) converted to metric scale using a haemocytometer.

Statistical analysis

Statistical analyses were performed using StatView v5.0 and Intercooled Stata v10. Data are presented as means \pm s.e.m. and were analyzed using one or two-factorial analysis of variance (ANOVA) with *Qkf-GFP* expression levels with or without the specific transgenic founder mouse line or the culture passage number as the independent factors followed by Fisher's or Bonferroni's post-hoc test. Pearson's regression analysis was carried out where appropriate, followed by a two-tailed *t*-test.

Acknowledgements

We thank C. Gatt, M. Becroft, T. McLennan, N. Downer and the WEHI FACS and Imaging laboratories for excellent technical support. We are grateful for the gift of the *eGFP* plasmid pLD53SCA-E-B from N. Heintz, for the β -actin-*GFP* transgenic mice from A. Nagy and the *Bmi1* mutant mice from M. van Lohuizen.

Funding

This work was supported by the Australian National Health and Medical Research Council (to T.T. and A.K.V.: project grants, senior research fellowships, Government IRISS; to B.N.S.: scholarship), the Australian Stem Cell Centre (to T.T. and A.K.V.: program module; to B.N.S.: scholarship), as well as by the Victorian Government through infrastructure support.

Supplementary material available online at

<http://jcs.biologists.org/lookup/suppl/doi:10.1242/jcs.077271/-/DC1>

References

- Aguiar, R. C., Chase, A., Coulthard, S., Macdonald, D. H., Carapeti, M., Reiter, A., Sohal, J., Lennard, A., Goldman, J. M. and Cross, N. C. (1997). Abnormalities of chromosome band 8p11 in leukemia: two clinical syndromes can be distinguished on the basis of MOZ involvement. *Blood* **90**, 3130-3135.

- Beckervordersandforth, R., Tripathi, P., Ninkovic, J., Bayam, E., Lepier, A., Stempflhuber, B., Kirchhoff, F., Hirrlinger, J., Haslinger, A., Lie, D. C. et al. (2010). In vivo fate mapping and expression analysis reveals molecular hallmarks of prospectively isolated adult neural stem cells. *Cell Stem Cell* **7**, 744-758.
- Bernstein, B. E., Mikkelsen, T. S., Xie, X., Kamal, M., Huebert, D. J., Cuff, J., Fry, B., Meissner, A., Wernig, M., Plath, K. et al. (2006). A bivalent chromatin structure marks key developmental genes in embryonic stem cells. *Cell* **125**, 315-326.
- Borrow, J., Stanton, V. P., Jr, Andresen, J. M., Becher, R., Behm, F. G., Chaganti, R. S., Civin, C. I., Distech, C., Dube, I., Frischau, A. M. et al. (1996). The translocation t(8;16)(p11;p13) of acute myeloid leukaemia fuses a putative acetyltransferase to the CREB-binding protein. *Nat. Genet.* **14**, 33-41.
- Calaora, V., Chazal, G., Nielsen, P. J., Rougon, G. and Moreau, H. (1996). mCD24 expression in the developing mouse brain and in zones of secondary neurogenesis in the adult. *Neuroscience* **73**, 581-594.
- Capela, A. and Temple, S. (2002). LeX/ssea-1 is expressed by adult mouse CNS stem cells, identifying them as nonpendymal. *Neuron* **35**, 865-875.
- Capela, A. and Temple, S. (2006). LeX is expressed by principle progenitor cells in the embryonic nervous system, is secreted into their environment and binds Wnt-1. *Dev. Biol.* **291**, 300-313.
- Carapeti, M., Aguiar, R. C., Goldman, J. M. and Cross, N. C. (1998). A novel fusion between MOZ and the nuclear receptor coactivator TIF2 in acute myeloid leukemia. *Blood* **91**, 3127-3133.
- Chaffanet, M., Mozziconacci, M. J., Fernandez, F., Sainy, D., Lafage-Pochitaloff, M., Birnbaum, D. and Pebusque, M. J. (1999). A case of inv(8)(p11q24) associated with acute myeloid leukemia involves the MOZ and CBP genes in a masked t(8;16). *Genes Chromosomes Cancer* **26**, 161-165.
- Chaffanet, M., Gressin, L., Preudhomme, C., Soenen-Cornu, V., Birnbaum, D. and Pebusque, M. J. (2000). MOZ is fused to p300 in an acute monocytic leukemia with t(8;22). *Genes Chromosomes Cancer* **28**, 138-144.
- Chiasson, B. J., Tropepe, V., Morshead, C. and van der Kooy, D. (1999). Adult mammalian forebrain ependymal and subependymal cells demonstrate proliferative potential, but only subependymal cells have neural stem cell characteristics. *J. Neurosci.* **19**, 4462-4471.
- Clayton-Smith, J., O'Sullivan, J., Daly, S., Bhaskar, S., Day, R., Anderson, B., Voss, A. K., Thomas, T., Biesecker, L. G., Smith, P. et al. (2011). Whole-exome-sequencing identifies mutations in histone acetyltransferase gene KAT6B in individuals with the Say-Barber-Biesecker variant of Ohdo syndrome. *Am. J. Hum. Genet.* **89**, 675-681.
- Coskun, V., Wu, H., Bianchi, B., Tsao, S., Kim, K., Zhao, J., Biancotti, J. C., Hutnick, L., Krueger, R. C., Jr, Fan, G. et al. (2008). CD133⁺ neural stem cells in the ependyma of mammalian postnatal forebrain. *Proc. Natl. Acad. Sci. USA* **105**, 1026-1031.
- Craig, C. G., D'sa, R., Morshead, C. M., Roach, A. and van der Kooy, D. (1999). Migrational analysis of the constitutively proliferating subependyma population in adult mouse forebrain. *Neuroscience* **93**, 1197-1206.
- Curtis, M. A., Penney, E. B., Pearson, A. G., van Roon-Mom, W. M., Butterworth, N. J., Dragunow, M., Connor, B. and Faull, R. L. (2003). Increased cell proliferation and neurogenesis in the adult human Huntington's disease brain. *Proc. Natl. Acad. Sci. USA* **100**, 9023-9027.
- Doetsch, F. and Alvarez-Buylla, A. (1996). Network of tangential pathways for neuronal migration in adult mammalian brain. *Proc. Natl. Acad. Sci. USA* **93**, 14895-1900.
- Doetsch, F., Garcia-Verdugo, J. M. and Alvarez-Buylla, A. (1997). Cellular composition and three-dimensional organization of the subventricular germinal zone in the adult mammalian brain. *J. Neurosci.* **17**, 5046-5061.
- Doetsch, F., Caille, L., Lim, D. A., Garcia-Verdugo, J. M. and Alvarez-Buylla, A. (1999). Subventricular zone astrocytes are neural stem cells in the adult mammalian brain. *Cell* **97**, 703-716.
- Esteyries, S., Perot, C., Adelaide, J., Imbert, M., Lagarde, A., Pautas, C., Olschwang, S., Birnbaum, D., Chaffanet, M. and Mozziconacci, M. J. (2008). NCOA3, a new fusion partner for MOZ/MYST3 in M5 acute myeloid leukemia. *Leukemia* **22**, 663-665.
- Garcia, A. D., Doan, N. B., Imura, T., Bush, T. G. and Sofroniew, M. V. (2004). GFAP-expressing progenitors are the principal source of constitutive neurogenesis in adult mouse forebrain. *Nat. Neurosci.* **7**, 1233-1241.
- Gong, S., Yang, X. W., Li, C. and Heintz, N. (2002). Highly efficient modification of bacterial artificial chromosomes (BACs) using novel shuttle vectors containing the R6Kgamma origin of replication. *Genome Res.* **12**, 1992-1998.
- Graham, V., Khudyakov, J., Ellis, P. and Pevny, L. (2003). SOX2 functions to maintain neural progenitor identity. *Neuron* **39**, 749-765.
- Hadjantonakis, A. K., Gertsenstein, M., Ikawa, M., Okabe, M. and Nagy, A. (1998). Generating green fluorescent mice by germline transmission of green fluorescent ES cells. *Mech. Dev.* **76**, 79-90.
- Imamura, T., Kakazu, N., Hibi, S., Morimoto, A., Fukushima, Y., Ijuin, I., Hada, S., Kitabayashi, I., Abe, T. and Imashuku, S. (2003). Rearrangement of the MOZ gene in pediatric therapy-related myelodysplastic syndrome with a novel chromosomal translocation t(2;8)(p23;p11). *Genes Chromosomes Cancer* **36**, 413-419.
- Jensen, J. B. and Parmar, M. (2006). Strengths and limitations of the neurosphere culture system. *Mol. Neurobiol.* **34**, 153-161.
- Katsumoto, T., Aikawa, Y., Iwama, A., Ueda, S., Ichikawa, H., Ochiya, T. and Kitabayashi, I. (2006). MOZ is essential for maintenance of hematopoietic stem cells. *Genes Dev.* **20**, 1321-1330.

- Kitabayashi, I., Aikawa, Y., Yokoyama, A., Hosoda, F., Nagai, M., Kakazu, N., Abe, T. and Ohki, M. (2001). Fusion of MOZ and p300 histone acetyltransferases in acute monocytic leukemia with a t(8;22)(p11;q13) chromosome translocation. *Leukemia* **15**, 89-94.
- Kondo, T. and Raff, M. (2004). Chromatin remodeling and histone modification in the conversion of oligodendrocyte precursors to neural stem cells. *Genes Dev.* **18**, 2963-2972.
- Kraft, M., Cirstea, I. C., Voss, A. K., Thomas, T., Goehring, I., Sheikh, B., Gordon, L., Scott, H., Smyth, G., Ahmadian, M. R. et al. (2011). Disruption of the histone acetyltransferase MYST4 leads to a Noonan syndrome-like phenotype and hyperactivated MAPK signaling. *J. Clin. Invest.* **121**, 3479-3491.
- Laywell, E. D., Rakic, P., Kukekov, V. G., Holland, E. C. and Steindler, D. A. (2000). Identification of a multipotent astrocytic stem cell in the immature and adult mouse brain. *Proc. Natl. Acad. Sci. USA* **97**, 13883-13888.
- Lois, C. and Alvarez-Buylla, A. (1993). Proliferating subventricular zone cells in the adult mammalian forebrain can differentiate into neurons and glia. *Proc. Natl. Acad. Sci. USA* **90**, 2074-2077.
- Lois, C., Garcia-Verdugo, J. M. and Alvarez-Buylla, A. (1996). Chain migration of neuronal precursors. *Science* **271**, 978-981.
- Louis, S. A., Rietze, R. L., Deleyrolle, L., Wagey, R. E., Thomas, T. E., Eaves, A. C. and Reynolds, B. A. (2008). Enumeration of neural stem and progenitor cells in the neural colony-forming cell assay. *Stem Cells* **26**, 988-996.
- Merson, T. D., Dixon, M. P., Collin, C., Rietze, R. L., Bartlett, P. F., Thomas, T. and Voss, A. K. (2006). The transcriptional coactivator Querkopf controls adult neurogenesis. *J. Neurosci.* **26**, 11359-11370.
- Mignone, J. L., Kukekov, V., Chiang, A. S., Steindler, D. and Enikolopov, G. (2004). Neural stem and progenitor cells in nestin-GFP transgenic mice. *J. Comp. Neurol.* **469**, 311-324.
- Mikkelsen, T. S., Ku, M., Jaffe, D. B., Issac, B., Lieberman, E., Giannoukos, G., Alvarez, P., Brockman, W., Kim, T. K., Koche, R. P. et al. (2007). Genome-wide maps of chromatin state in pluripotent and lineage-committed cells. *Nature* **448**, 553-560.
- Mirzadeh, Z., Merkle, F. T., Soriano-Navarro, M., Garcia-Verdugo, J. M. and Alvarez-Buylla, A. (2008). Neural stem cells confer unique pinwheel architecture to the ventricular surface in neurogenic regions of the adult brain. *Cell Stem Cell* **3**, 265-278.
- Mirzadeh, Z., Doetsch, F., Sawamoto, K., Wichterle, H. and Alvarez-Buylla, A. (2010). The subventricular zone en-face: wholemount staining and ependymal flow. *J. Vis. Exp.* **6**, 1938.
- Molofsky, A. V., Pardal, R., Iwashita, T., Park, I. K., Clarke, M. F. and Morrison, S. J. (2003). Bmi-1 dependence distinguishes neural stem cell self-renewal from progenitor proliferation. *Nature* **425**, 962-967.
- Morshead, C. M., Craig, C. G. and van der Kooy, D. (1998). In vivo clonal analyses reveal the properties of endogenous neural stem cell proliferation in the adult mammalian forebrain. *Development* **125**, 2251-2261.
- Morshead, C. M., Garcia, A. D., Sofroniew, M. V. and van der Kooy, D. (2003a). The ablation of glial fibrillary acidic protein-positive cells from the adult central nervous system results in the loss of forebrain neural stem cells but not retinal stem cells. *Eur. J. Neurosci.* **18**, 76-84.
- Morshead, C. M., Garcia, A. D., Sofroniew, M. V. and van der Kooy, D. (2003b). The ablation of glial fibrillary acidic protein-positive cells from the adult central nervous system results in the loss of forebrain neural stem cells but not retinal stem cells. *Eur. J. Neurosci.* **18**, 76-84.
- Nam, H. S. and Benezra, R. (2009). High levels of Id1 expression define B1 type adult neural stem cells. *Cell Stem Cell* **5**, 515-526.
- Panagopoulos, I., Fioretos, T., Isaksson, M., Samuelsson, U., Billstrom, R., Strombeck, B., Mitelman, F. and Johansson, B. (2001). Fusion of the MORF and CBP genes in acute myeloid leukemia with the t(10;16)(q22;p13). *Hum. Mol. Genet.* **10**, 395-404.
- Pastrana, E., Cheng, L. C. and Doetsch, F. (2009). Simultaneous prospective purification of adult subventricular zone neural stem cells and their progeny. *Proc. Natl. Acad. Sci. USA* **106**, 6387-6392.
- Perez-Campo, F. M., Borrow, J., Kouskoff, V. and Lacaud, G. (2009). The histone acetyl transferase activity of monocytic leukemia zinc finger is critical for the proliferation of hematopoietic precursors. *Blood* **113**, 4866-4874.
- Potten, C. S. and Loeffler, M. (1990). Stem cells: attributes, cycles, spirals, pitfalls and uncertainties. Lessons for and from the crypt. *Development* **110**, 1001-1020.
- Reynolds, B. A. and Weiss, S. (1992). Generation of neurons and astrocytes from isolated cells of the adult mammalian central nervous system. *Science* **255**, 1707-1710.
- Reynolds, B. A. and Rietze, R. L. (2005). Neural stem cells and neurospheres – re-evaluating the relationship. *Nat. Methods* **2**, 333-336.
- Rietze, R. L., Valcanis, H., Brooker, G. F., Thomas, T., Voss, A. K. and Bartlett, P. F. (2001). Purification of a pluripotent neural stem cell from the adult mouse brain. *Nature* **412**, 736-739.
- Rozman, M., Camos, M., Colomer, D., Villamor, N., Esteve, J., Costa, D., Carrio, A., Aymerich, M., Aguilar, J. L., Domingo, A. et al. (2004). Type I MOZ/CBP (MYST3/CREBBP) is the most common chimeric transcript in acute myeloid leukemia with t(8;16)(p11;p13) translocation. *Genes Chromosomes Cancer* **40**, 140-145.
- Shen, Q., Wang, Y., Kokovay, E., Lin, G., Chuang, S. M., Goderie, S. K., Roysam, B. and Temple, S. (2008). Adult SVZ stem cells lie in a vascular niche: a quantitative analysis of niche cell-cell interactions. *Cell Stem Cell* **3**, 289-300.
- Thomas, T. and Voss, A. K. (2007). The diverse biological roles of MYST histone acetyltransferase family proteins. *Cell Cycle* **6**, 696-704.
- Thomas, T., Voss, A. K., Chowdhury, K. and Gruss, P. (2000). Querkopf, a MYST family histone acetyltransferase, is required for normal cerebral cortex development. *Development* **127**, 2537-2548.
- Thomas, T., Corcoran, L. M., Gugasyan, R., Dixon, M. P., Brodnicki, T., Nutt, S. L., Metcalf, D. and Voss, A. K. (2006). Monocytic leukemia zinc finger protein is essential for the development of long-term reconstituting hematopoietic stem cells. *Genes Dev.* **20**, 1175-1186.
- Vizmanos, J. L., Larrayoz, M. J., Lahortiga, I., Floristan, F., Alvarez, C., Otero, M. D., Novo, F. J. and Calasanz, M. J. (2003). t(10;16)(q22;p13) and MORF-CREBBP fusion is a recurrent event in acute myeloid leukemia. *Genes Chromosomes Cancer* **36**, 402-405.
- Voss, A. K. and Thomas, T. (2009). MYST family histone acetyltransferases take center stage in stem cells and development. *BioEssays* **31**, 1050-1061.
- Voss, A. K., Krebs, D. L. and Thomas, T. (2006). C3G regulates the size of the cerebral cortex neural precursor population. *EMBO J.* **25**, 3652-3663.
- Voss, A. K., Collin, C., Dixon, M. P. and Thomas, T. (2009). Moz and retinoic acid coordinately regulate H3K9 acetylation, Hox gene expression, and segment identity. *Dev. Cell* **17**, 674-686.
- Wang, Z., Zang, C., Cui, K., Schones, D. E., Barski, A., Peng, W. and Zhao, K. (2009). Genome-wide mapping of HATs and HDACs reveals distinct functions in active and inactive genes. *Cell* **138**, 1019-1031.
- Ware, C. B., Wang, L., Mecham, B. H., Shen, L., Nelson, A. M., Bar, M., Lamba, D. A., Dauphin, D. S., Buckingham, B., Askari, B. et al. (2009). Histone deacetylase inhibition elicits an evolutionarily conserved self-renewal program in embryonic stem cells. *Cell Stem Cell* **4**, 359-369.
- Zhao, C., Deng, W. and Gage, F. H. (2008). Mechanisms and functional implications of adult neurogenesis. *Cell* **132**, 645-660.